This article has been accepted for publication in a future issue of this journal, but has not been fully edited. Content may change prior to final publication. Citation information: DOI 10.1109/JLT.2021.3121467, Journal of Lightwave Technology

480 Gbps WDM Transmission Through an $Al_2O_3:Er^{3+}$ Waveguide Amplifier

T. Chrysostomidis, I. Roumpos, K. Fotiadis, J. Mu, A. Manolis, C. Vagionas, M. Dijkstra, S.M. Garcia Blanco, T. Alexoudi, and K. Vyrsokinos

***Abstract*—The increasing need for more efficient communication networks has been the main driving force for the development of complex photonic integration circuits combining active and passive building blocks towards advanced functionality. However, this perpetual effort comes with the cost of additive power losses and the research community has resorted to the investigation of different materials to establish efficient on-chip amplification. Among the different proposals, erbium-doped waveguide amplifiers appear to be a promising solution for high performance transmission in the C-band band with low fabrication cost, due to their CMOS compatibility and integration potential with the silicon\silicon nitride photonic platforms. In this paper we provide a holistic study for high-speed WDM transmission capabilities of a monolithically integrated $Al_2O_3:Er^{3+}$ spiral waveguide amplifier co-integrated with Si_3N_4 components, providing a static characterization and a dynamic evaluation for (a) 4×40 Gbps, (b) 8×40 Gbps and (c) 8×60 Gbps WDM transmissions achieving clearly open eye diagram in all cases. The active region of the erbium doped waveguide amplifier consists of a 5.9 cm $Al_2O_3:Er^{3+}$ spiral adiabatically coupled to passive Si_3N_4 waveguides combined with on chip 980 nm/1550 nm WDM Multiplexers/Demultiplexers. Experimental results reveal bit-error rate values below the KR4-FEC limit of 2×10^{-5} for all channels, without any DSP applied on the transmitter or receiver side for a 4×40 Gbps and 8×40 Gbps data stream transmission.**

***Index Terms*— Erbium, Optical amplifiers, Wavelength division multiplexing, Monolithic integrated circuits.**

I. Introduction

THE advent of erbium doped amplifiers has boosted the deployment of fiber optic networks and unleashed wavelength division multiplexing (WDM) technology for transfer of multi-Tbps data streams over long distances. Photonic integrated circuits (PICs) improve the performance of these networks and lower their cost by introducing in the transmission and routing of the WDM channels silicon photonics based available integrated components, like filters, polarization handling and mode manipulation devices [1]. This technology transfer was achieved after the rapid evolution of silicon photonics performance that triggered a subsequent increase in the number of integrated components per circuit for more advanced functionality. However, that in turn yielded a growing number of total losses that brought to surface the need for on-chip amplification targeting neutral loss per PIC like electronic integrated circuits. In this direction photonic integration follows two major research paths for the realization of on-chip amplifiers, i.e. the Semiconductor Optical Amplifiers (SOAs) and the erbium doped waveguide amplifiers (EDWAs) [2][3][4].

The progress in photonics technology has enabled the co-integration of SOAs with the silicon platform via hybrid and heterogeneous techniques [5], and transfer printing [6]. However, these methods add extra fabrication steps, such as III-V material bonding and film transfer [2] with direct penalty to overall PIC cost. In addition, they also limit the maximum thermal budget applied on the wafer for advanced back end of line post processing [7]. Another main disadvantage of SOAs in terms of amplification performance comes from the short lifetime of the upper level carriers, associating the SOAs with undesirable large gain compression and pattern effects, especially at multi tens of Gbaud line rates. As a result, all these SOAs' nonlinearities cause severe signal degradations that dictate the appliance of heavy digital signal processing (DSP) at the receiver side [8] for signal regeneration.

On the other side, EDWAs are widely studied and tested for a large set of substrate materials, erbium ion hosts and active region geometries [4], targeting to maximize the net gain in the smallest possible area. In the silicon photonics platform especially, promising results have been delivered from EDWAs in terms of gain [9], bandwidth, and noise figure [10] with performance now being close to Er^{+3} fibre based amplifiers. Table I presents an overview of the different types of Er^{3+} integrated amplifiers presented so far in the literature covering different integration techniques. The record value in net gain per unit length is 20.1 dB/cm [9] from a slot waveguide with

Manuscript received XXX XX, XX; revised XX XX, XX; accepted XXXX XX, XX. This work has received funding from the Hellenic Foundation for Research and Innovation, General Secretariat for Research and Technology through the ORION (GA No 585) and the Stichting voor de Technische Wetenschappen (STW) (STW-13536) and in part by the European Research Council (ERC) (GA No 648978).

T. Chrysostomidis, I. Roumpos and K. Vyrsokinos are with the Department of Physics and Center for Interdisciplinary Research and Innovation, Aristotle University of Thessaloniki, 57001, Greece. (e-mail: tchrysos@auth.gr, ioroumpo@auth.gr, kv@auth.gr)

K. Fotiadis, A. Manolis, C. Vagionas and T. Alexoudi are with the Department of Informatics and Center for Interdisciplinary Research and Innovation, Aristotle University of Thessaloniki, 57001, Greece. (e-mail: kfotiadi@csd.auth.gr, athanasm@csd.auth.gr, chvagion@csd.auth.gr, theonial@csd.csd.gr)

J. Mu, M. Dijkstra, and S.M. Garcia Blanco are with the Integrated Optical Systems (IOS) Group, MESA+ Institute for Nanotechnology, University of Twente, P.O Box 217, 7500 AE, Enschede, The Netherlands. (e-mail: jinfeng.mu@icloud.com, m.dijkstra@utwente.nl, s.m.garciablanco@utwente.nl)

This article has been accepted for publication in a future issue of this journal, but has not been fully edited. Content may change prior to final publication. Citation information: DOI 10.1109/JLT.2021.3121467, Journal of Lightwave Technology

TABLE I
Comparison of integrated amplifiers on silicon photonic platform

PIC-fiber interface	Net Gain [dB/cm]	Er^{3+} hosting platform and WG type	Active Region Length [cm]	Rate [Gbps]	Ref.
Si_3N_4	20.1	Al_2O_3: Straight channel	0.12	-	[9]
Al_2O_3:Er^{3+}	1.55	Al_2O_3: Spiral channel	12.9	-	[10]
Al_2O_3:Er^{3+}	1.92	Al_2O_3: Straight channel	5.7	170	[11]
Al_2O_3:Er^{3+}	1.7	Al_2O_3: Straight channel	5.4	-	[12]
Si_3N_4	1.8	Al_2O_3: Spiral channel	10	-	[13]
Al_2O_3:Er^{3+}	7 dB SE	Al_2O_3: Spiral channel	0.95	-	[14]
Si_3N_4 coated with Al_2O_3:Er^{3+}	2.8	Al_2O_3: Straight channel	0.12/ 0.16	-	[15]
Si_3N_4 coated with TeO_2:Er^{3+}	1.7	TeO_2: Paperclip shaped	2.2	-	[16]
Er:LNOI	5	LNOI: Spiral channel	3.6	-	[17]
Er:LNOI	6.2	LNOI: Spiral channel	2.58	-	[18]
Si_3N_4	**1.44**	**Al_2O_3: Spiral channel**	**5.9**	**480**	**[This work]**

only 1.2 mm length. An alternative approach is of straight or spiral Al_2O_3:Er^{3+} active regions [10]–[14] exhibiting a net gain in the range of 1.5 dB/cm to 1.92 dB/cm. A simpler EDWA integration technology, exploits a passive waveguide from Si_3N_4 coated with the erbium doped material [9], [15], [16] and a hybrid mode is propagating across the two layers. With this configuration up to 2.8 dB/cm net gain has been measured, but again the length of the device was short. Finally, a different hosting material for Er doping is Thin Film Lithium Niobate on Insulator (TFLNOI) platform exhibiting waveguide gain of 5 dB/cm [17] and 6.2 dB/cm [18].

From Table I, it also comes into surface that the Si_3N_4 is gaining traction as the most suitable hosting platform for the Al_2O_3:Er^{3+} based integrated amplifiers, due to the low substrate cost, the availability of a variety of building blocks and the very low losses in the fiber-PIC interfaces going down to 0.5 dB [19]. In addition, these amplifiers could be monolithically co-integrated on the same silicon chip with transceivers and compensate the losses of additional components and subsystems for advanced processing with reduced assembly cost, in comparison to interconnected standalone fiber pigtailed units. This research path has been demonstrated in [18], where the EWDA compensates the losses of a reconfigurable optical add-drop multiplexer fabricated also on the Si_3N_4 waveguide platform. In terms of transmission capabilities though, up until now the highest data transmission rate reported in an EDWA reaches 170 Gbps [11], but this was on a single channel. Demonstrations of high aggregated capacity with WDM transmission credentials are currently missing, limiting in this way the practicality of the Er^{3+} based integrated amplifiers in modern transmission systems.

In this paper, we demonstrate for the first time to the best of our knowledge, the WDM transmission capabilities of an EDWA chip with the active region of Al_2O_3:Er^{3+} monolithically integrated on the Si_3N_4 platform. Three scenarios of gradually increased aggregate rates are examined, starting from 4×40 Gbps, then proceeding to 8×40 Gbps and finally testing the chip with 8×60 Gbps. Clear eye diagrams are recorded with minimum signal distortion due to EDWA amplification for all three cases and error free bit error rate (BER) curves under forward error correction (FEC) for the first two scenarios. The BER penalty versus the same line without the EDWA chip is less than 0.9 dB and 1.0 dB for the KR4-FEC limit under the 4×40 Gbps and 8×40 Gbps transmissions, respectively. Due to constraints in the bandwidth of the photodiode and the error detector it was not possible to take BER for the 60 Gbps line rate. Under static conditions, the Al_2O_3:Er^{3+} active region exhibits signal enhancement (SE) and net gain of 29.3 dB and 8.5 dB. Unfortunately, due to the high losses of the fiber to chip interfaces from the absence of PIC inverse taper mode converters, the net gain of the entire chip was negative.

The continuation of this work is organized as follows: Section II presents the layout and the process for the fabrication of the PIC and describes the static characterization results. Section III is devoted to the characterization of the EDWA chip in the three WDM scenarios of 4×40 Gbps, 8×40 Gbps and 8×60 Gbps with a complete set of spectra and eye diagrams. For the first two we present also BER curves for confirmation of the high quality of the transmitted signal. Finally, section IV summarizes the paper.

II. EDWA Chip Description

Fig. 1 presents a schematic overview of the on-chip amplifier layout comprised of the passive Si_3N_4 and active Al_2O_3:Er^{3+} layers. The device features two input/ two output ports for fiber-PIC light coupling, offering the option of C-band signal and 980 nm pump multiplexing (MUX) either on chip with Si_3N_4 multi-mode interference (MMI) couplers or externally with fiber WDM couplers. The fiber to chip interfaces imposed 10 dB and 12 dB coupling losses for the signal and pump wavelength, respectively, as there were no inverse tapers for proper mode transformation. However, there are reports that this value can be as low as 0.5 dB/interface [19]. The losses of the MUX/DEMUX MMIs were approximately 1.7 dB for signal port and 8.3 dB for pump port at 1550 nm (C-band), while at 980 nm the same port induced 2.7 dB losses.

The Si_3N_4 waveguides were fabricated by low pressure

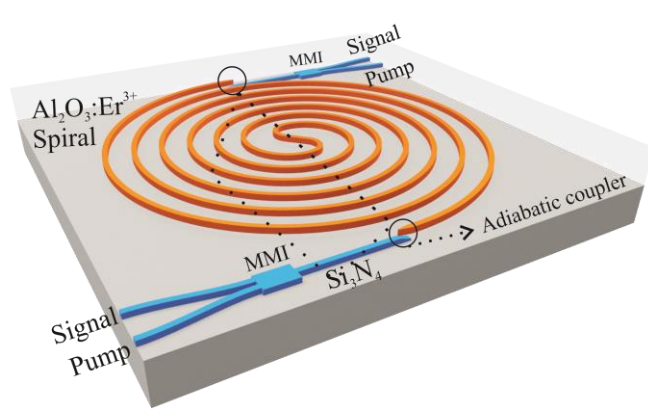

Fig. 1 Chip layout, consisting of input/output pump and signal facets, MMI couplers, vertical adiabatic couplers between the passive Si_3N_4 and active region. Blue Si_3N_4 layer, orange Al_2O_3:Er^{3+} layer.

chemical vapor deposition (LPCVD) followed by UV contact lithography and reactive ion etching (RIE) with CHF_3 and O_2 chemistry. The propagation losses were experimentally measured to be 0.14 dB/cm at 1532 nm for a cross-sectional dimensions of 1.4 µm width and 200 nm thickness. The monomode Al_2O_3 waveguides were fabricated by depositing using RF magnetron sputtering followed by UV contact lithography and RIE. Their dimensions were 800 nm thick and 1.4 µm wide. The Al_2O_3 waveguides were doped with erbium, with a targeted concentration of 1.7×10^{20} cm^{-3} by RF reactive co-sputtering. Vertical adiabatic couplers [20],[13], were utilized to transfer the light from the Si_3N_4 waveguide to the active Al_2O_3 spiral and back to the passive Si_3N_4, inducing 0.5 dB losses per transition according to a reference die with 2-6-12 cascaded structures from the same wafer. In the adiabatic coupler the Si_3N_4 waveguide is vertically tapered from 200 nm to 30 nm, while the Al_2O_3 waveguide is horizontally tapered from 1.4 µm to 800 nm. The active layer was design for monomode operation at signal and pump wavelength under transverse electric (TE) polarization in agreement with the design optimization of the MMI MUXs/DEMUXs. The length of the Al_2O_3:Er^{3+} spiral was 5.9 cm for this experiment and more details about the fabrication process can be found in [13], [20], [21].

For the characterization of the chip initially an optimized experimental setup was employed, where the pump and the signal were injected to the chip via a dual window 980 nm / 1550 nm fiber array and the mixing was performed at the MMIs. In addition, a diphenyl index matching liquid was dropped to the fiber-PIC interface for reduction of the already high losses. However, due to the evaporation of the liquid, the array was shifting position, and the optical alignment was becoming unstable after a short period of time preventing the recording of the measurements in a consistent manner. For this reason, the signal and the pump were MUXed externally and then injected via a polarization maintaining fiber (PMF) with a FC/PC connector through the pump port of the MMI MUX, targeting to achieve maximum pump power at the active region for optimized performance. This approach was much more stable in terms of fiber-PIC coupling and the extra losses of the signal could be compensated with an external EDFA in the following transmission experiments. The total losses of the signal/pump from the fiber to the Al_2O_3:Er^{3+} spiral was estimated at 18.8/15.2 dB with a breakdown of 10/12 dB for the coupling interface, 8.3/2.7 dB for the MMI coupler and 0.5/0.5 dB for the adiabatic coupler, respectively.

Fig. 2(a) illustrates the experimental setup for the evaluation of the SE of the EDWA chip, with SE calculated as the difference in the measured power of the continuous waveform (CW) signal at the output of the chip after being filtered, when the 980 nm co-propagating pump is ON and OFF. It should be noted that the measured SE does not account for any fiber chip coupling and waveguide losses and provides a simple metric for identifying the gain capabilities of the Er^{3+} doped waveguide [4]. The CW signal is generated by a tunable semiconductor laser (TSL) providing adjustable output power and frequency, while the 980 nm pump light is coming from a butterfly

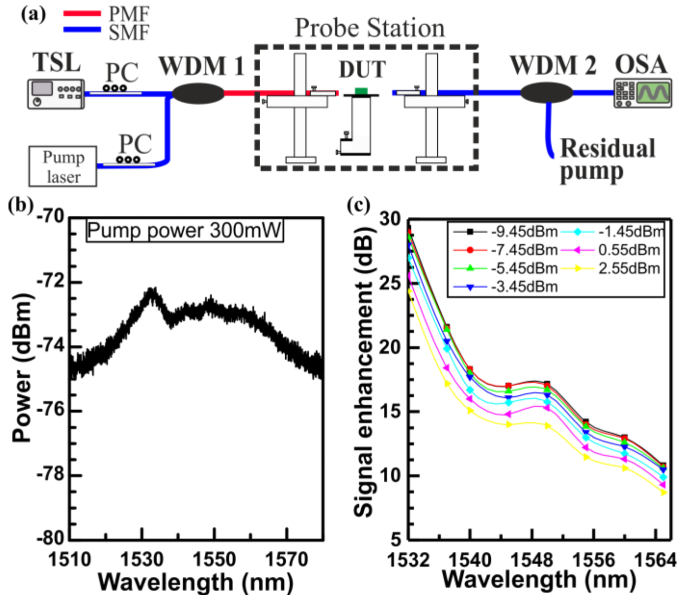

Fig. 2(a) Experimental setup for signal enhancement measurements at C-band wavelengths [1532 nm – 1565 nm]. (b) The ASE spectrum with only the pump laser on and no signal input. (c) Calculated (curves) and measured (data points) values of signal enhancement as a function of the input power versus the wavelength. input signal power range between -9.45 dBm and 2.55 dBm with co-propagating pump light chip incident power of 300 mW at 980 nm.

packaged commercial module delivering 300 mW output power measured after WDM coupler 1. According to the previous loss calculations, the power of the pump reaching the active region is approximately 9 mW. The 980 nm/1550 nm coupled signal from the fiber WDM coupler is then injected to the chip with the PMF employed for optimum signal launching conditions in terms of recorded SE. At the output of the chip (DUT), the signal is collected with a single mode fiber (SMF) and filtered by means of another WDM coupler to reject the remaining pump light. The filtered output is then inserted to the optical spectrum analyzer (OSA) and recorded for further analysis in terms of SE and amplified spontaneous emission (ASE) shape.

Fig. 2(b) presents the ASE spectrum of the EDWA for maximum pump power incident at the chip, revealing a similar shape with Er^{+3} doped fiber amplifiers, whereas Fig. 2(c) illustrates the CW SE measurements in the region of 1532 nm to 1565 nm with a step of 3 and 5 nm for variable signal input powers. The graph reveals a peak of 29.3 dB at 1532 nm in agreement with typical (gain) ASE curves from Er^{3+} doped amplifiers. At 1550 nm the SE is in the region of 15-17 dB, while at 1565 nm there is still a significant SE of around 10 dB. The power at the input of the chip was varied in all measurements from -9.45 dBm up to 2.55 dBm corresponding to -28.45 dBm and -16.45 dBm launched power at Al_2O_3:Er^{3+} spiral, respectively. Also, it should be pointed out that by adjusting the input power of the chip to below -10 dBm, then the 30 dB SE benchmarks could easily be obtained for 1532 nm. For the same chip it was measured also the net gain of the active region that is defined as the actual CW light measured output power minus the actual measured input power, plus the in/out fiber to active region calculated losses. For a spiral input power of -28 dBm (light saturation region) and -10 dBm (deep saturation region) the total net gain was calculated to 8.5 dB and 6.5 dB respectively. By dividing these values to the 5.9 cm

This article has been accepted for publication in a future issue of this journal, but has not been fully edited. Content may change prior to final publication. Citation information: DOI 10.1109/JLT.2021.3121467, Journal of Lightwave Technology

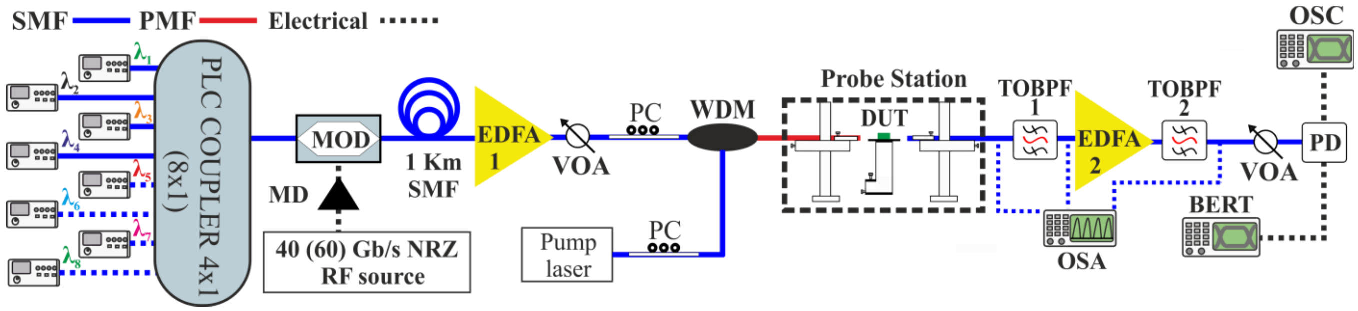

Fig. 3 The experimental setup used for the 4×40(8×40-8×60) Gbps NRZ transmission evaluation. **MOD**: Modulator, **NRZ:** Non-Return to Zero, **MD:** Modulator Driver, **EDFA:** Erbium Doped Fiber Amplifier, **VOA:** Variable Optical Attenuator, **PC:** Polarization Controller, **WDM**: WDM 1550/980 nm coupler, T**OBPF: Tunable** Optical Bandpass Filter, **SMF**: Single mode fiber, **PMF:** Polarization Maintaining Fiber, **PD:** Photodiode, **OSC:** Oscilloscope, **BERT:** Bit Error Rate Tester, **DUT:** Device Under Test.

length of the spiral, the results are 1.44 dB/cm and 1.10 dB/cm gain, with similar values reported also from a passive characterization of a similar fabricated chip for a 10 cm long $Al_2O_3:Er^{3+}$ spiral [13]. For these two input powers the net losses of the chip were measured to 22.9 and 24.9 dB, respectively.

III. WDM Transmission Experiments with Co-propagating Pump on the EDWA Chip

The following sub-sections demonstrate the experimental results of A) 4×40 Gbps B) 8×40 Gbps and C) 8×60 Gbps WDM data stream transmission through the on-chip amplifier utilizing a co-propagating 980 nm pump laser. Each sub-section consist of a WDM data stream SE evaluation, WDM transmission eye diagrams and for cases A) and B) BER curves with and without the chip to show the degradation on the signal quality caused by the EDWA chip and the spectra of each channel after demultiplexing at the output of the setup.

A. 4×40 Gpbs WDM Transmission

The EDWA chip was initially employed in a WDM 4×40 Gbps data transmission setup with the Er^{3+} doped spiral pumped in a co-propagating configuration of 300 mW chip incident power. Fig. 3 presents the detailed experimental set up with four distributed feedback lasers (DFB) generating the four CW signals an λ_1 = 1549 nm, λ_2 = 1550.50 nm, λ_3 = 1552 nm, and λ_4 = 1553.50 nm multiplexed by a 4×1 wavelength insensitive planar lightwave circuit (PLC) coupler. The WDM signal was then modulated by a programmable pattern generator (PPG) with a pseudo random binary sequence (PRBS7) through a $LiNbO_3$ Mach-Zehnder modulator (MOD). The decorrelation of the WDM signals was ensured through the insertion of 1 Km SMF in the transmission line inducing 24 ps time delay between the channels. EDFA 1 was placed at the output of the SMF for compensation of the expected high input fiber to PIC interface losses and boosted the power of the WDM signal at 12 dBm max power for operation of the EDWA under heavy saturation. Precise polarization and total power of the WDM stream injected to the chip were adjusted by a PC and a variable optical attenuator (VOA), respectively. An extra PC was inserted at the setup for controlling the polarization of the pump light and afterwards it was combined with the WDM stream in the same way as for the SE measurements. The common output was delivered then to the chip via a PM fiber providing stabilized launching conditions. At the EDWA output a SMF was placed for monitoring the output signal amplified through the EDWA spiral with an OSA at the signal port as shown in Fig. 1. The polarization of all signals i.e., WDM stream and 980 nm pump was adjusted for maximum SE monitored with the OSA. A wavelength tunable optical bandpass filter (TOBPF) 1 with 1 nm 3-dB bandwidth (BW) was inserted in the line after the chip for i) rejection of Amplified Spontaneous Emission (ASE) noise ii) isolation of the transmitted signal from the pump laser remained from the on-chip WDM coupler and iii) demultiplexing of the WDM stream to single channels for subsequent channel evaluation. The opto-electric (OE) conversion of the signal was achieved through a 40 GHz photodiode (PD) featuring 38 GHz 3-dB OE bandwidth. The error detector required a minimum 3.5 dBm power inserted in the PD for 10^{-9} BER and around 0 dBm for BER of 2×10^{-5} that is the KR4-FEC limit. For this reason, EDFA 2 was introduced in the experimental setup to partially compensate the losses from the output fiber PIC interfaces and amplify the power coming out of the chip to the desired levels.

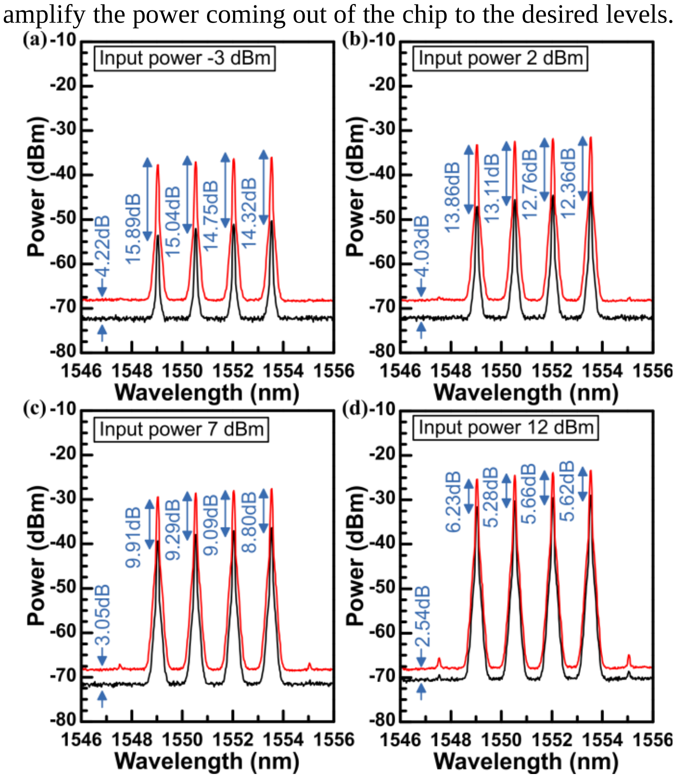

Fig. 4. Optical spectra of the four-channel signal (1549 nm, 1550.5 nm, 1552 nm, 1553.5 nm) captured after the EDWA chip with total input signal power at the chip (a) -3 dBm, (b) 2 dBm, (c) 7 dBm, (d) 12 dBm. Black and red line corresponds to pump laser being OFF and ON. The double ended arrow indicates the signal enhancement of every channel. Also, at the bottom left of every diagram the enhancement of the noise level is being pointed out. The OSA resolution of 0.1 nm.

This article has been accepted for publication in a future issue of this journal, but has not been fully edited. Content may change prior to final publication. Citation information: DOI 10.1109/JLT.2021.3121467, Journal of Lightwave Technology

The ASE noise of the EDFA 2 was filtered out by a second tunable TOBPF 2 with 1 nm 3-dB BW. A second VOA adjusted the input optical power injected to the PD. The final signal passing through the two EDFAs and the EDWA was monitored simultaneously at the digital sampling oscilloscope (OSC) and at the BER tester (BERT).

Fig. 4(a)-(d) show the recorded spectra obtained directly at the output of the chip when the pump is ON and OFF for a variable total chip input power with 5 dBm step of -3 dBm, 2 dBm, 7 dBm and 12 dBm. The double ended arrow on each graph illustrates the measured SE for each channel. For the lowest input power of -3dBm (Fig. 4(a)) the SE is ranging from 14.32 dB to 15.89 dB, as the channel wavelength is moving from 1553.5 nm to 1549 nm. The ASE noise floor is also raised by 4.22 dB for these conditions. When the input power was increased to 2 dBm (Fig. 4(b)), the SE varied between 12.36 dB and 13.86 dB for all four channels and the ASE noise floor was enhanced by 4.03 dB. At 7 dBm total input power (Fig. 4(c), the SE was measured to be between 8.80 dB and 9.91 dB with the ASE noise floor raised now by 3.05 dB. Finally, as Fig. 4(d) illustrates, at the maximum input power of 12 dBm the EDWA chip was still providing a SE in the range of 5.28 dB to 6.23 dB for all four channels and the noise floor was increased by 2.54 dB.

Fig. 5(a)-(b) present the back to back (BtB) optical eye diagrams of the 1549.0 nm and 1550.5 nm channel of the WDM signal measured when the EWDA the chip was replaced by a VOA that adjusted the power of each channel to the corresponding value at output power of OPBF1, when the chip was in the line. The BtB eye diagrams of the remaining two channels were almost identical to the ones of Fig. 5(a), (b) and are omitted for space saving. Fig. 5(c)-(f) show the eye diagrams of the transmitted signal at the output of EDFA 2 for 12 dBm total incident signal power at the chip input with vertical eye opening (VEO) of 4.3 dB, 4.0 dB, 4.3 dB and 4.5 dB for the four channels at 1549 nm, 1550.5 nm, 1552 nm, and 1553.5 nm, respectively. The vertical opening of the eye diagram is defined as the comparison of the 3σ "one" and 3σ "zero" levels and indicates the worst case Extinction Ratio. The corresponding eye opening for the BtB channels were 4.5 dB, 4.4 dB, 4.5 dB, 4.7 dB, revealing only a slight signal degradation for each one of the four channels.

The very high signal quality is confirmed also with results of Fig. 6, where solid lines depict the BER curves of the signal passing through the EDWA spiral, whereas the dashed lines the corresponding BtB ones. The horizontal dashed line denotes the threshold for the KR4-FEC of 2×10^{-5} for NRZ signals, where minimum BER of all signals exceed by far the requirement for

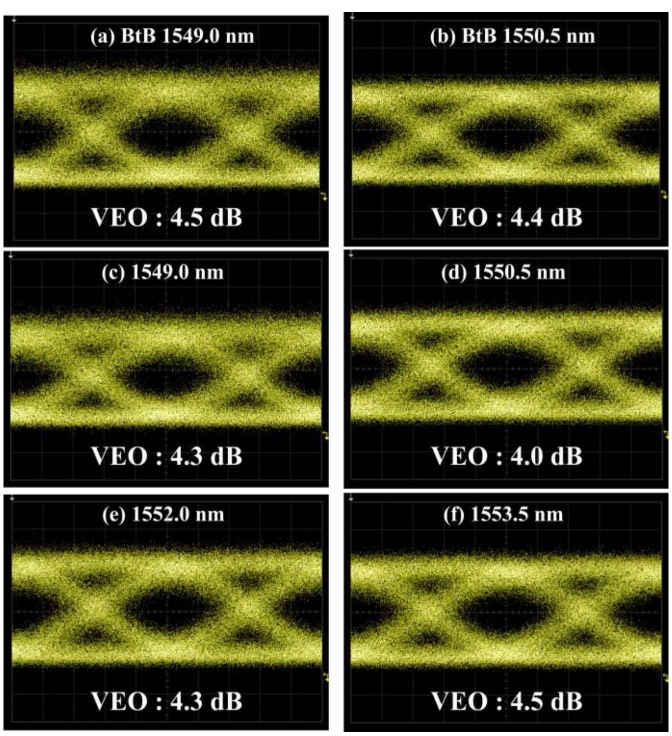

Fig. 5 Transmission eye diagrams for: (a) BtB λ_1, (b) BtB λ_2, (c) λ_1, (d) λ_2, (e) λ_3, (f) λ_4. In all diagrams the scaling is 5ps/div and 6.3mV/div in the horizontal and vertical axis, respectively.

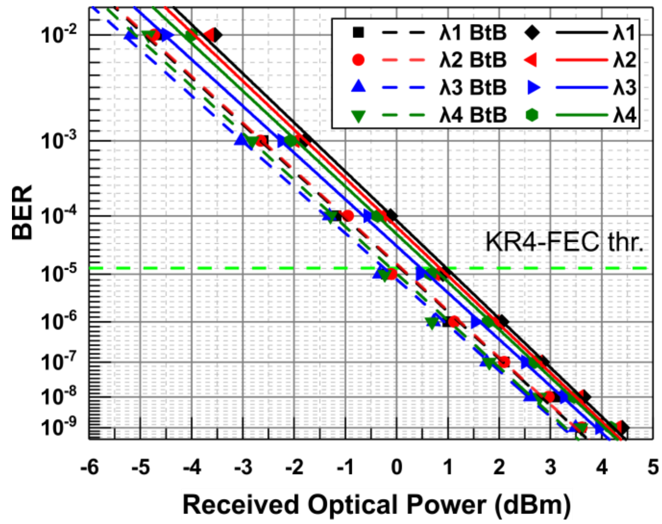

Fig. 6 BER measurements for the 4×40 Gbps transmission with EDWA and BtB.

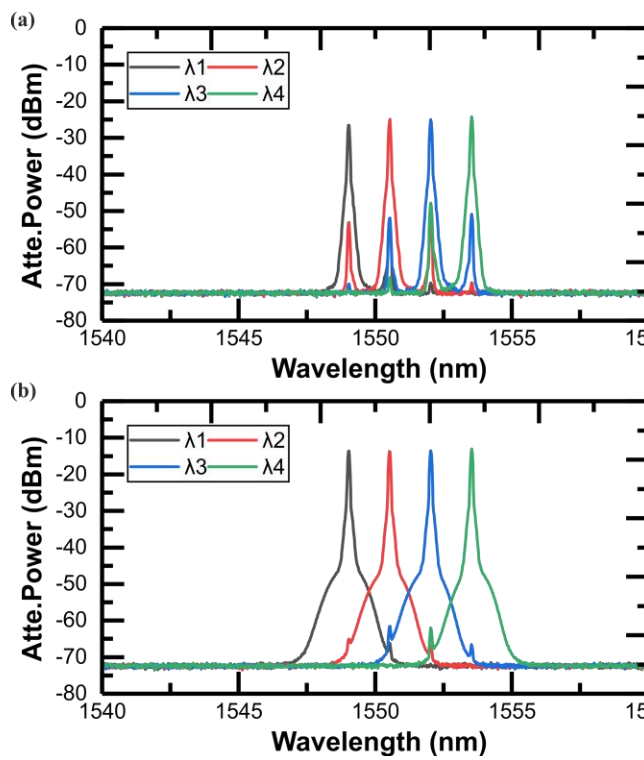

Fig. 7 Overlay of isolated spectra after TOBPF 1 (a) & 2 (b).The OSA resolution of 0.1 nm.

This article has been accepted for publication in a future issue of this journal, but has not been fully edited. Content may change prior to final publication. Citation information: DOI 10.1109/JLT.2021.3121467, Journal of Lightwave Technology

error free transmission under FEC. The power penalty at FEC limit was of 0.9 dB for 1549 nm, 0.75 dB for 1550.5nm, 0.7 dB for 1552 nm and 0.7 dB for 1553, while the minimum BER was for all channels in the order of 10^{-9}. These BER values were achieved without any DSP at the recorded signals.

Fig. 7(a) shows the overlayed diagrams of the isolated spectra for each channel after TOBPF 1 filtering, revealing an adjacent channel suppression of more than 30 dB for each one, in agreement with the Fig. 5 eye diagrams where no channel crosstalk is present. The measured power for each channel with a power meter at this point was: -21.4 dBm, -19.8 dBm, -19.8 dBm, -18.81 dBm, from λ_1 to λ_4 channel, respectively. Fig. 7(b) presents the combined spectra after each channel has been amplified at EDFA 2 and filtered at TOBPF 2. The spectra of Fig. 7(b) shows that each channel is super positioned on a high in band noise peak accumulated mainly from EDFA 2 due to the low power coming out of the chip and this noise is the main source of signal degradation during final evaluation.

B. 8×40 Gbps WDM Transmission

After the successful evaluation of the EDWA chip with the 4×40 Gbps WDM transmission, the setup was extended for the amplification of an 8×40 Gbps stream with the corresponding experimental layout depicted in Fig. 3. The only change versus the four-channel transmission is the incorporation of four extra DFB lasers resulting in total eight CW carriers at λ_1 = 1545.50 nm, λ_2 = 1547.10 nm, λ_3 = 1548.70 nm, λ_4 = 1550.30 nm, λ_5 = 1551.90 nm, λ_6 = 1553.60 nm, λ_7 = 1555.20 nm, and λ_8 = 1556.80 nm. The eight signals are MUXed with an 8×1 wavelength insensitive PLC coupler and the output is injected to the LiNbO3 Mach-Zehnder MOD for the generation of an eight channel WDM data stream that followed the same transmission line and evaluation methods as in sub-section A.

Fig. 8(a)-(d) depict the recorded spectra of the WDM stream when the pump in ON/OFF state for a variable total input power in the range of -2.75 dBm to 15.36 dBm with a step of ~6 dB that brings the operation of the EDWA from the light to the deep saturate regime, respectively. Again, the double ended arrow on each graph illustrates the measured SE for each channel. For the minimum power of -2.75 dBm (Fig. 8(a)) the SE is between 12.68 dB and 15.88 dB, while the ASE level is now increased by 3.3 dB for the ON state. These are similar values to the ones obtained with the 4×40 Gbps transmission and confirm that the

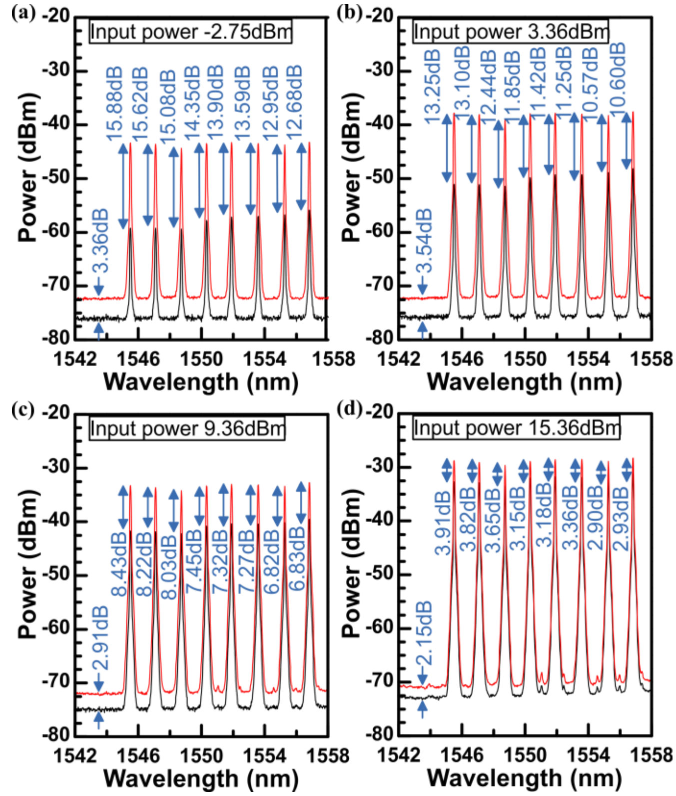

Fig. 8 Optical spectra of the eight-channel signal (1545.50 nm, 1547.10 nm, 1548.70 nm, 1550.30 nm, 1551.90 nm, 1553.50, 1555.20 nm, 1556.80 nm) captured after the EDWA chip with total input signal power at the chip (a) -2.75 dBm, (b) 3.36 dBm, (c) 9.36 dBm, (d) 15.36 dBm. Black and red line corresponds to pump laser being OFF and ON. The double ended arrow indicates the signal enhancement of every channel. Also, at the bottom left of every diagram the enhancement of the noise level is being pointed out. The OSA resolution of 0.1 nm.

EDWA is only lightly saturated under these conditions. For the maximum injected power of 15.36 dBm (Fig. 8(d)), the SE from the EDWA is between 2.93 dB and 3.91 dB, with these values now being almost 3dB lower than the ones for the 4×40 Gbps experiment (Fig. 4(d)) and verifying the deep saturation of the EDWA. The noise floor is raised by 2.15 dB, slightly lower than the 4×40 Gbps amplification. Also, a small variation of 1.3 dB in the SE is observed among the eight transmitted channels. It is important to note also that going from -2.75 dBm to 3.36 dBm input power, the SE drops only ~2 dB per channel. However, for the next two cases i.e., going from 3.36 dBm to 9.36 dBm and from 9.36 dBm to 15.36 dBm, the SE is reduced by ~4 dB,

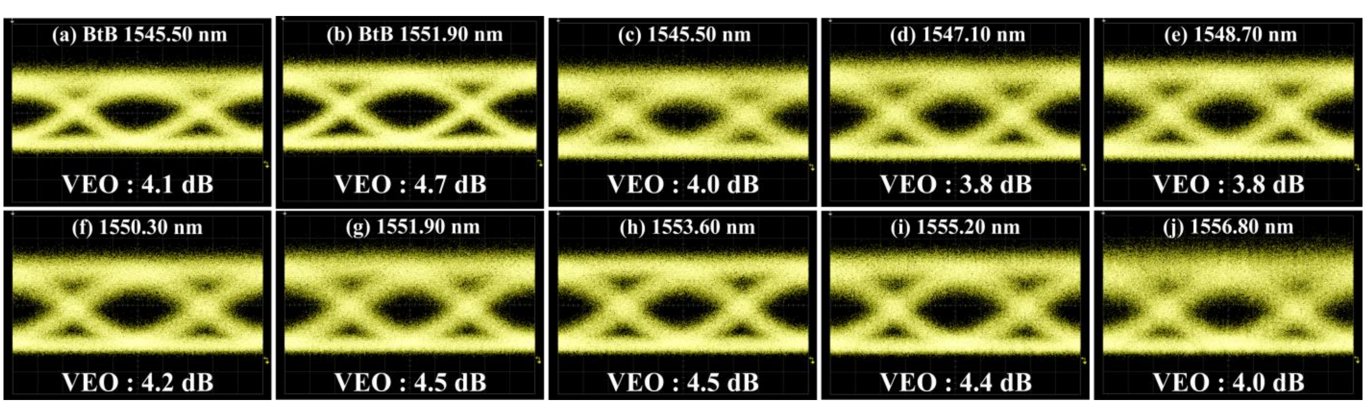

Fig. 9: 8×40 transmission eye diagrams for: (a) BtB λ_1, (b) BtB λ_5, (c) λ_1, (d) λ_2, (e) λ_3, (f) λ_4, (g) λ_5, (h) λ_6, (i) λ_7, and (j) λ_8. In all diagrams the scaling is 5ps/div and 6.3mV/div in the horizontal and vertical axis, respectively.

This article has been accepted for publication in a future issue of this journal, but has not been fully edited. Content may change prior to final publication. Citation information: DOI 10.1109/JLT.2021.3121467, Journal of Lightwave Technology

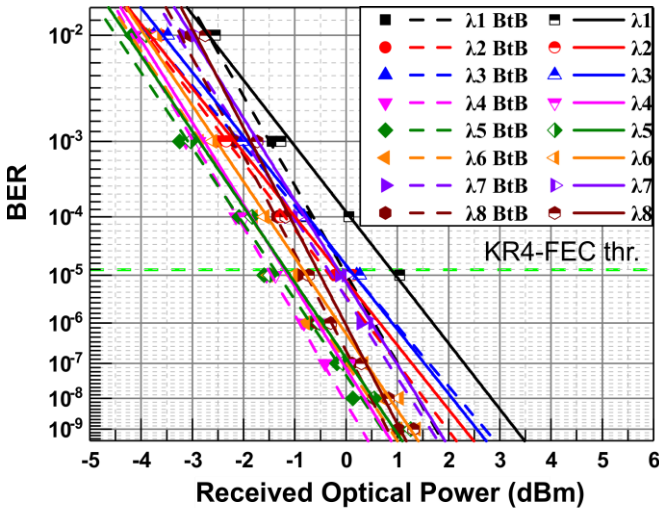

Fig. 10 Back to back and normal BER measurements for the 8×40 Gbps transmission.

revealing that strong saturation starts at around 3.5 dBm chip input power. The SE per channel for 3.36dBm input power is in the range of 10.6 dB - 13.25 dB, while for 9.36 dBm input power it is between 6.83 dB - 8.43 dB. The SE variation among the channels is due to the spectral gain dependance from the combination of EDFA1 and EDWA.

Fig. 9 depict the eye diagrams of the amplified NRZ signals at 40 Gbps as obtained at the output of TOBPF 2 with the OSC for every channel for the maximum input power of 15.36 dBm at the EDWA input. Fig. 9(a) and (b) presents the BtB eye of the first channel at 1545 nm and one of the middle ones at 1551.9 nm, and as in IV section the remaining eyes of the other six ones exhibited similar performance and are omitted for space saving. Fig. 9(c)-(j) illustrate the eye diagrams of the EDWA transmitted data streams with each channel featuring a vertical eye opening of 4.0 dB, 3.8 dB, 3.8 dB, 4.2 dB, 4.5 dB, 4.5 dB, 4.4 dB, 4.0 dB for λ_1 to λ_8, respectively. The corresponding eye opening for the BtB channels were 4.1 dB, 3.9 dB, 4.0 dB, 4.3 dB, 4.7 dB, 4.6 dB, 4.6 dB, 4.4 dB, revealing again only a very small signal quality degradation for each one of the eight channels.

Fig. 10 illustrates the BER values of the stream transmitted through the EDWA. Each channel achieved different minimum error-rate value ranging in the order of 10^{-5} for 1545.5 nm, 1547.1 nm, and 1548.7 nm, 10^{-6} for 1555,2 nm, 10^{-7} for 1550.3 nm and 10^{-9} for 1551.9 nm, 1553.6 nm, and 1556.8 nm. The different error floor is a result of the non-flat gain profile of the three cascaded Er^{+3} doped amplifiers. It should be pointed out that an error floor on the same level is appearing also for the back-to-back (VOA) transmission, so any signal degradation for these wavelengths is coming from the whole link and not exclusively from the EDWA chip. However, even with this 8-channel stress test, the bit error rate floor remains above the KR4-FEC threshold with power penalty 0.93 dB, 0.24 dB, 0.1 dB, 0.32 dB, 0.23 dB, 0.37 dB, 0.18 dB, 0.28 dB for λ_1 to λ_8, respectively. Again, it should be mentioned no digital signal processing was applied on the transmitter or receiver side. The lowest performance for the three first channels is due to the dip in the gain of the EDWA at this spectral region as it is confirmed from the ASE spectrum of Fig. 8(a).

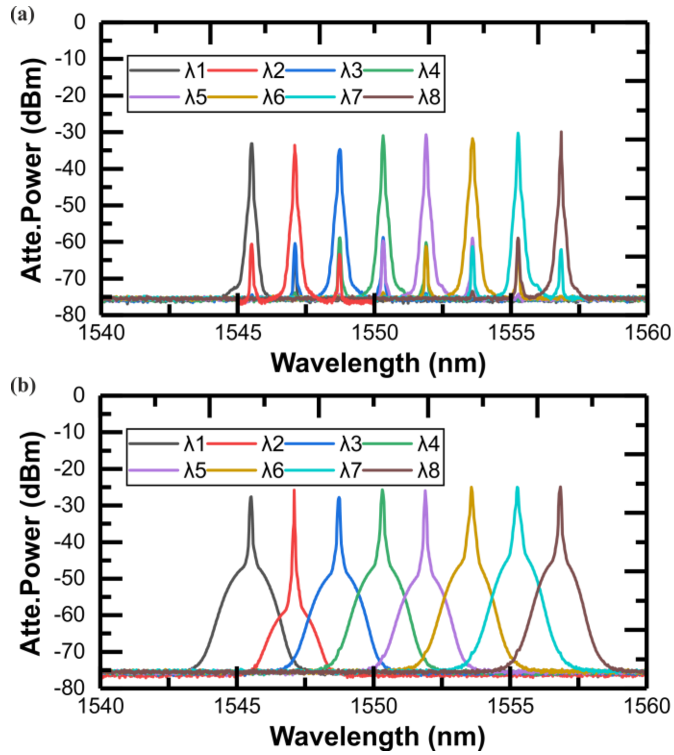

Fig. 11 Overlay of isolated spectra after TOBPF 1 & 2.The OSA resolution of 0.1 nm.

Fig. 11(a) shows the overlayed diagrams of the isolated spectra for each channel after TOBPF 1 filtering, indicating an adjacent channel suppression of more than 30 dB for each one, agreeing with the Fig. 9 eye diagrams where no channel crosstalk is present. The measured power for each channel at this point was: -24.2 dBm, -24.6 dBm, -26.2 dBm, -22 dBm, -21.8 dBm, -22.8 dBm, -21.3 dBm, -20.7 dBm. Fig. 11(b) presents the combined spectra after each channel has been amplified at EDFA 2 and filtered at TOBPF 2 and reveals that each channel is super positioned on a high in-band noise peak accumulated mainly from EDFA 2 due to signal's low power coming out of the EDWA chip and is the main origin for signal degradation and the obtained BER error floors.

C. 8×60 Gbps WDM Transmission

The proposed EDWA chip was also experimentally evaluated in an 8×60 Gbps WDM transmission scenario targeting maximum achievable aggregated data rate with the available equipment in the laboratory. The set up employed for this experiment follows the same fashion as reported in the previous cases descripted in Sections B and C and can be viewed at Fig. 3 but features two differences. The 40 Gbps Pulse Pattern Generator of the BER Tester is replaced by an arbitrary waveform generator (AWG) featuring 100 GS/s and ~ 40 GHz analog bandwidth. Also, the 1-nm tunable filters are exchanged with 3-nm bandwidth for accommodation of the higher line rate per channel. Fig. 12 depict the eye diagrams obtained for the generated NRZ signals at 60 Gbps as obtained at OSC for each one of the eight wavelengths plus the two BtB eye diagrams from λ_1=1545 nm and λ_5=1551.9 nm. The average optical power of the WDM data stream before entering the chip was 15.5 dBm, while the power of the modulated signals at the λ_1-λ_8 wavelengths emerging at the output of the chip were -17.2 dBm, -17 dBm, -16.8 dBm, -16.9 dBm, -16.3 dBm,

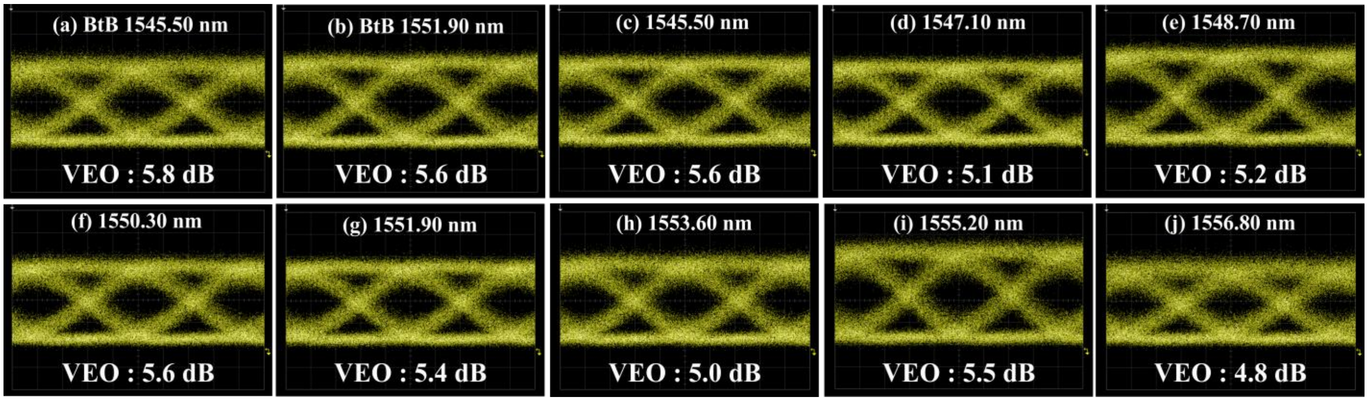

Fig. 12 8×60 transmission eye diagrams for: (a) BtB λ_1, (b)BtB λ_5, (c) λ_1, (d) λ_2, (e) λ_3, (f) λ_4, (g) λ_5, (h) λ_6, (i) λ_7, and (j) λ_8. In all diagrams the scaling is 5ps/div and 6.3mV/div in the horizontal and vertical axis, respectively.

-16.6 dBm, -16.5 dBm and -20.75 dBm, respectively. The higher power versus the 40 Gbps/channel transmission is coming from the wider tunable filters at the output of the PIC. The vertical eye opening of Fig. 12 were measured above 5.6 dB, 5.1 dB, 5.2 dB, 5.6 dB, 5.4 dB, 5.0 dB, 5.5 dB and 4.8 dB for all channels with the improved performance coming from the better quality of the electrical driving signal at the transmitter. The corresponding BtB values were 5.8 dB, 5.3 dB, 5.4 dB, 5.8 dB, 5.6 dB, 5.1 dB, 5.7 dB and 5.0 dB. Due to the limited BW of the error detector in the BER tester, it was not possible to perform BER measurements at 60 Gbps, but the clear and open eye diagrams of Fig. 12 indicate that the KR4-FEC limit would be easily obtainable. Again, no DSP was applied for enhanced signal quality at the transmitter or receiver side. So overall, the EDWA PIC is capable to amplify a 480 Gbps aggregate traffic stream without any significant drop in the signal quality.

Although, the device currently provides a net loss, its overall performance can be drastically improved by including spot size converters [19], for reduced fiber-PIC coupling losses and increasing the length of the spiral to more than 10 cm as in [13]. With these improvements it is expected a net gain for more than 7 dB at low saturation for the compensation of other components losses. The replacement also of the photodiode in the experimental setup with an avalanche photoreceiver as in [22], will enable the elimination of any other external fiber amplifier in the point-to-point link towards handling and routing of WDM streams entirely through Si_3N_4 based PICs. Finally, optimization of the pump laser delivery to the active region in terms of coupling losses, could allow the simultaneous amplification of 16 or even 32 channels.

IV. Conclusions

We have demonstrated a 4×40, 8×40 and 8×60 Gbps WDM data stream transmission through an EDWA device featuring a 5.9 cm long Al_2O_3:Er^{3+} active region spiral, monolithically co-integrated with a Si_3N_4 layer providing the fiber-PIC interfaces and the 980 nm-1550 nm MUXs/DEMUXs. In static characterization amplification of a CW light at 1532 nm revealed 29.3 dB SE and 1.44 dB/cm spiral net gain for -9.45 dBm incident signal input power to the chip. For the 4×40 Gbps transmission evaluation, the eye diagrams at the output of the setup demonstrated a vertical eye opening between 4.0 dB to 4.5 dB with only a slight distortion compared to the BtB scenario. The corresponding BER curves revealed error free transmission for all channels with power penalty between 0.7-0.9 dB at the KR4-FEC threshold. In the 8×40 Gbps transmission, the vertical open eye diagrams were in the range of 3.8 dB to 4.5 dB and the BER power penalty vs. the KR4-FEC threshold was between 0.1 dB to 0.9 dB for all eight channels. The 8×60 Gbps transmission was performed with a high performance AWG instead of the PPG of the BER Tester as electrical data source and the vertical eye openings of the eight channels at the output of the experimental setup were in the range of 4.8 dB to 5.6 dB. Due to the limited BW of the error detector in the BER tester, it was not possible to perform BER measurements at 60 Gbps, but the clear and open eye diagrams indicate that the KR4-FEC limit would be easily reachable again with even lower power penalty vs. the two 40 Gbps/channel experiments. The EDWA chip imposed a net loss due to the high losses from the chip fiber interfaces, but with improvements in the design and fabrication the proposed device is suitable for processing high capacity WDM streams in lossless Si_3N_4 based PICs featuring advanced functionality.

References

[1] Y. Su, Y. Zhang, C. Qiu, X. Guo, and L. Sun, "Silicon Photonic Platform for Passive Waveguide Devices: Materials, Fabrication, and Applications," *Adv. Mater. Technol.*, vol. 5, no. 8, pp. 1–19, 2020, doi: 10.1002/admt.201901153.

[2] P. Zhou, B. Wang, X. Wang, B. Wang, Y. He, and J. Bowers, "An on-chip electrically driven, position-adapted, fully integrated erbium-based waveguide amplifier for silicon photonics," *OSA Contin.*, vol. 4, no. 3, pp. 790–814, 2021, doi: 10.1364/osac.413492.

[3] D. R. Zimmerman and L. H. Spiekman, "Amplifiers for the Masses: EDFA, EDWA, and SOA Amplets for Metro and Access Applications," *J. Light. Technol.*, vol. 22, no. 1, pp. 63–70, 2004, doi: 10.1109/JLT.2003.822144.

[4] J. D. B. Bradley and M. Pollnau, "Erbium-doped integrated waveguide amplifiers and lasers," *Laser Photonics Rev.*, vol. 5, no. 3, pp. 368–403, 2011, doi: 10.1002/lpor.201000015.

[5] P. Kaspar *et al.*, "Hybrid III-V/silicon SOA for photonic integrated circuits," *Nanophotonics Micro/Nano Opt. II*, vol. 9277, p. 927708, 2014, doi:

10.1117/12.2074617.

[6] B. Corbett, R. Loi, J. O'Callaghan, and G. Roelkens, "Chapter Three - Transfer Printing for Silicon Photonics," in *Silicon Photonics*, vol. 99, S. Lourdudoss, R. T. Chen, and C. Jagadish, Eds. Elsevier, 2018, pp. 43–70.

[7] M. Smit, K. Williams, and J. Van Der Tol, "Past, present, and future of InP-based photonic integration," *APL Photonics*, vol. 4, no. 5, 2019, doi: 10.1063/1.5087862.

[8] A. Arnould *et al.*, "Experimental Characterization of Nonlinear Distortions of Semiconductor Optical Amplifiers in the WDM Regime," *J. Light. Technol.*, vol. 38, no. 2, pp. 509–513, 2020, doi: 10.1109/JLT.2019.2950147.

[9] J. Rönn *et al.*, "Ultra-high on-chip optical gain in erbium-based hybrid slot waveguides," *Nat. Commun.*, vol. 10, no. 1, pp. 1–9, 2019, doi: 10.1038/s41467-019-08369-w.

[10] S. A. Vázquez-Córdova *et al.*, "Erbium-doped spiral amplifiers with 20 dB of net gain on silicon," *Opt. Express*, vol. 22, no. 21, p. 25993, 2014, doi: 10.1364/oe.22.025993.

[11] J. D. B. Bradley *et al.*, "170 Gbit/s transmission in an erbium-doped waveguide amplifier on silicon," *Opt. Express*, vol. 17, no. 24, p. 22201, 2009, doi: 10.1364/oe.17.022201.

[12] J. D. B. Bradley, L. Agazzi, D. Geskus, F. Ay, K. Wörhoff, and M. Pollnau, "Gain bandwidth of 80 nm and 2 dB/cm peak gain in Al_2O_3:Er^3+ optical amplifiers on silicon," *J. Opt. Soc. Am. B*, vol. 27, no. 2, p. 187, 2010, doi: 10.1364/josab.27.000187.

[13] J. Mu, M. Dijkstra, J. Korterik, H. Offerhaus, and S. M. García-Blanco, " High-gain waveguide amplifiers in Si 3 N 4 technology via double-layer monolithic integration ," *Photonics Res.*, vol. 8, no. 10, p. 1634, 2020, doi: 10.1364/prj.401055.

[14] L. Agazzi *et al.*, "Monolithic integration of erbium-doped amplifiers with silicon-on-insulator waveguides," *Opt. Express*, vol. 18, no. 26, p. 27703, 2010, doi: 10.1364/oe.18.027703.

[15] J. Rönn *et al.*, "Erbium-doped hybrid waveguide amplifiers with net optical gain on a fully industrial 300 mm silicon nitride photonic platform," *Opt. Express*, vol. 28, no. 19, p. 27919, 2020, doi: 10.1364/oe.399257.

[16] H. C. Frankis *et al.*, " Erbium-doped TeO 2 -coated Si 3 N 4 waveguide amplifiers with 5 dB net gain ," *Photonics Res.*, vol. 8, no. 2, p. 127, 2020, doi: 10.1364/prj.8.000127.

[17] J. Zhou *et al.*, "On-Chip Integrated Waveguide Amplifiers on Erbium-Doped Thin-Film Lithium Niobate on Insulator," *Laser Photonics Rev.*, vol. 15, no. 8, 2021, doi: 10.1002/lpor.202100030.

[18] M. Cai *et al.*, "Erbium-doped lithium niobate thin film waveguide amplifier with 16 dB internal net gain," vol. 1, pp. 0–7, 2021.

[19] C. G. H. Roeloffzen *et al.*, "Low-Loss Si3N4 TriPleX Optical Waveguides: Technology and Applications Overview," *IEEE J. Sel. Top. Quantum Electron.*, vol. 24, no. 4, pp. 1–21, 2018, doi: 10.1109/JSTQE.2018.2793945.

[20] J. Mu, M. DIjkstra, Y. S. Yong, M. De Goede, L. Chang, and S. M. García-Blanco, "Monolithic Integration of Al2O3 and Si3N4 Toward Double-Layer Active-Passive Platform," *IEEE J. Sel. Top. Quantum Electron.*, vol. 25, no. 5, 2019, doi: 10.1109/JSTQE.2019.2908559.

[21] J. Mu, M. DIjkstra, and S. M. García-Blanco, "Resonant Coupling for Active-Passive Monolithic Integration of Al2O3 and Si3N4," *IEEE Photonics Technol. Lett.*, vol. 31, no. 10, pp. 771–774, 2019, doi: 10.1109/LPT.2019.2907535.

[22] S. A. Srinivasan *et al.*, "56 Gb/s NRZ O-Band Hybrid BiCMOS-Silicon Photonics Receiver Using Ge/si Avalanche Photodiode," *J. Light. Technol.*, vol. 39, no. 5, pp. 1409–1415, 2021, doi: 10.1109/JLT.2020.3038361.